

Characterization of $\text{LiNi}_{0.8}\text{Mn}_{0.1}\text{Co}_{0.1}\text{O}_2$ (NMC 811) synthesized by molten salt assisted solid-state reaction

Yazid Rijal Azinuddin¹, Agus Purwanto^{1,2*}, and Arif Jumari^{1,2}

¹Department of Chemical Engineering, Faculty of Engineering, Universitas Sebelas Maret, Surakarta, 57126, Indonesia

²Centre of Excellence for Electrical Energy Storage Technology, Universitas Sebelas Maret, Surakarta, 57146, Indonesia

Abstract. The synthesis of Nickel manganese cobalt (NMC 811) cathode material was studied by comparing the molten salt method and the simple solid-state method. The use of easily decomposed raw materials such as metal oxalate and metal carbonate was further reviewed to determine their effect on the phase purity, crystallinity, and morphology of the NMC 811 material. XRD analysis showed that the material with metal oxalate and the solid-state method (NMC811 S-C2O4) had a hexagonal α - NaFeO_2 structure (space group R-3m) with few impurities that are close to the results of commercial NMC 811 material. While samples with metal carbonate (NMC811 S-CO3 and NMC811 M-CO3) detected more impurity phases one of them is Li_2CO_3 . In addition, the ideal structure has not been achieved. SEM results show that raw materials with metal carbonate produce less regular structures, while metal oxalate raw materials produce more uniform spherical primary particles. The molten salt method improves particle homogeneity but faces obstacles in removing impurities due to imperfect washing. These findings emphasize the importance of selecting precursors and synthesis methods to optimize the structural and morphological properties of NMC 811. Optimization of the washing protocol is needed in further research for better molten salt synthesis results. Further studies involving electrochemical performance tests, such as charge–discharge cycling and electrochemical impedance spectroscopy (EIS), are required to fully evaluate the synthesized materials.

1 Introduction

Lithium-ion batteries (LIBs) have advantages such as high energy density, high conversion efficiency, and long cycle life. Research on cathode materials plays a critical role in the development of lithium-ion battery (LIB) technology. The cathodes commonly used in lithium-ion batteries are lithium Nickel Manganese Cobalt oxide (NMC), lithium Nickel Cobalt Aluminium oxide (NCA) and Lithium Manganese Oxide (LMO). Currently, the most

*Corresponding author: aguspurwanto@staff.uns.ac.id

successful lithium-ion batteries are those that use a combination of nickel-manganese-cobalt (NMC) cathode materials. This battery has a synergistic effect of Ni, Co, and Mn, which makes NMC a new type of energy storage material with high specific capacity and high capacity retention ratio [1]. The NMC cathode has a Li_xMO_2 structure type layered (M = metal), with space group R-3m and lattice parameters $a \sim 2.8 \text{ \AA}$ and $c \sim 14 \text{ \AA}$ [2]. NMC has advantages, namely, high capacity, high heat and current stability, relatively high volume capacity and long cycle life.

The electrochemical performance of cathode materials strongly depends on the synthesis method, which governs crystallinity, phase purity, particle morphology, particle size, and cation mixing within the layered structure. Various methods have been applied to synthesize cathodes with high nickel content such as the solid-state, molten salt, co-precipitation method, combustion, and sol-gel. However, NMC materials with high nickel content are more difficult to synthesize with consistent quality due to the difficulty in oxidizing Ni^{2+} to Ni^{3+} perfectly, even in a pure O_2 atmosphere [3]. Incomplete oxidation will eventually lead to impurities, cation mixing and lithium deficiency, which will significantly affect the structural and electrochemical properties of the material. Therefore, to obtain a cathode material with a high nickel content and good electrochemical performance, it is necessary to conduct research on the synthesis/preparation method of NMC and the selection of the type of raw materials used.

The types of raw materials used in NMC production determine the process selection. Meanwhile, the formation technique for metal oxide materials such as NMC cathodes requires thermal decomposition of precursor materials. Materials that do not decompose within the NMC formation temperature range must be reacted through a series of processes to form compounds that readily decompose at the NMC formation temperature. Processes involving the formation of metal oxides requires easily decomposed materials. Easily decomposed materials include metal hydroxides, metal oxalates and metal carbonates [4][5][6][7][8]. Commonly used raw materials include metal hydroxides, metal oxalates, and metal carbonates. Metal hydroxides are a common form of metal used in industry due to their advantages and low cost. However, the potential for Na/K contamination, the need for special pH controls, and the lower tap density have prompted researchers to conduct further studies on other types of metals, such as metal oxalates and metal carbonates [9].

Metal carbonate compounds have been widely utilized as precursor materials due to their high chemical stability and compatibility with industrial-scale synthesis processes [10]. However, the thermal decomposition of carbonate precursors during calcination is accompanied by the evolution of CO_2 gas, which may induce the formation of porous microstructures and hinder effective particle densification, particularly in Ni-rich NMC cathode materials [11]. In comparison, metal oxalate precursors generally decompose through a more controlled thermal pathway, enabling improved regulation of stoichiometry and enhanced elemental homogeneity within the resulting material [12]. Previous studies have reported that oxalate-derived precursors can promote the formation of finer particles with more uniform morphologies, which are advantageous for lithium-ion transport and contribute to improved electrochemical stability [13].

The solid-state method is one of the simplest methods compared to other methods. NMC synthesis using this method solid-state reaction resulting in irregular particles, and a wider size distribution [14]. Molten salt is a synthesis method with a basic solid-state concept. Synthesis molten salt has been considered as a new method for synthesizing NMC cathodes, where molten salt can be used as both a solvent and a reactant [15]. Molten salt functions as a solvent for ionic liquids above the eutectic temperature, where the reactants dissolve easily and move rapidly, thus shortening reaction times. Several studies have shown the molten salt method to be promising. The molten salt method has the advantage of producing more

homogeneous particles and a narrow particle distribution. However, this method requires a large amount of washing water.

To date, the majority of published work has examined oxalate- or carbonate-derived precursors independently, typically within a single synthesis strategy. However, a systematic and side by side evaluation of oxalate and carbonate based precursors across different synthesis routes particularly solid-state and molten-salt methods for Ni-rich NMC 811 remains absent from the literature. This gap in comparative insight hinders the informed selection of appropriate precursor processing combinations for achieving optimal NMC cathode performance. Therefore, this study aims to systematically investigate the effects of precursor type (oxalate vs carbonate) and synthesis route (solid-state vs molten salt) on the phase purity, crystallinity, and morphology of NMC 811. To the best of the authors' knowledge, a direct comparison of oxalate- and carbonate-based precursors using both solid-state and molten salt routes has not been systematically reported.

2 Materials and Methods

2.1 Materials

The materials used are nickel oxalate (99.0%, Shandong China), manganese oxalate ($\geq 99\%$, Tercents India), and cobalt oxalate (99%, Penjing Chemical, China) for the metal oxalates. For the metal carbonates, nickel carbonate (98%, Epoch China), manganese carbonate (43.5%, Anhui China), and cobalt carbonate (46%, Shandong China) were used. Lithium hydroxide, $\text{LiOH}\cdot\text{H}_2\text{O}$ ($\geq 99\%$), was also used for the lithiation process from Leverton India.

2.2 NMC cathode material preparation process

The preparation of NMC cathode material using the solid-state method begins with the first stage, which is weighing nickel oxalate, manganese oxalate, and cobalt oxalate with a molar ratio of (8:1:1) for the experiments based on metal oxalate raw materials. Separately, the weighing of nickel carbonate, manganese carbonate, and cobalt carbonate with a molar ratio of (8:1:1) for experiments based on metal carbonate raw materials is also performed as the first stage. The second stage then involves the addition of lithium hydroxide ($\text{LiOH}\cdot\text{H}_2\text{O}$) with a molar ratio of (1:1.05) to compensate for lithium loss during high-temperature calcination. This ratio of lithium hydroxide addition is based on optimization results from previous research.

The grinding process was carried out using zirconia balls (10 mm diameter) at a rotational speed of 300 rpm in ambient air atmosphere. The ball to powder weight ratio was set at 10:1. Zirconia grinding containers were used to avoid metal contamination. Metal oxalates and metal carbonates were each combined with lithium hydroxide and then ground using a ball mill for 1 hour. For the molten salt method, NaCl salt was added with a salt-to-material weight ratio of 1:1 (w/w). This ratio was chosen to ensure sufficient formation of a liquid phase to enhance mass transport while maintaining ease of salt removal after synthesis. The solid-state method does not involve the addition of NaCl salt.

The mixed powder was calcined in an alumina crucible inside a tube furnace at a temperature of 600°C for 6 hours, with a heating rate of $10^\circ\text{C}/\text{min}$ under a flowing oxygen atmosphere (3 L/min). It was then cooled naturally inside the furnace to room temperature. The calcined sample was subsequently sintered at a temperature of 820°C for 12 hours, with a heating rate of $10^\circ\text{C}/\text{min}$ under a flowing oxygen atmosphere (3 L/min), to obtain the final layered NMC phase.

For samples from the molten salt method, the sintered product was washed repeatedly with deionized water to remove residual NaCl. Each washing cycle was performed using a solid-to-water mass ratio of 1:10 under magnetic stirring for 10 minutes. Washing was repeated until the conductivity of the supernatant fell below $10 \mu\text{S cm}^{-1}$, indicating effective removal of NaCl. The washed powder was then dried at 100°C for 12 hours. Each produced sample is designated as: solid-state metal oxalate method (NMC 811 S-C2O4), solid-state metal carbonate method (NMC 811 S-CO3), molten salt metal oxalate method (NMC 811 M-C2O4), and molten salt metal carbonate method (NMC 811 M-CO3). The process is shown in Figure 1, a schematic of material preparation for the solid-state and molten salt methods.

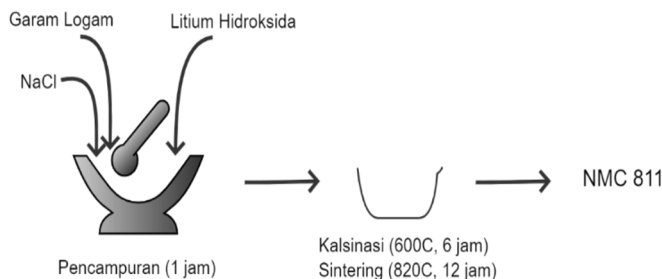


Fig. 1. Material Preparation for The Solid-State and Molten Salt Methods

2.3 Characterization of NMC Cathode

Characterization testing using FTIR (Fourier Transform Infrared Spectroscopy), XRD (X-Ray Diffractometer), and SEM (Scanning Electron Microscopy) was used to investigate the crystallinity, functional groups and morphology of the material. Japan. The crystal structure of the product was analyzed using EQ-MD-10-LD Precision Mini XRD using $\text{Cu K}\alpha$ radiation $\lambda = 1.54 \text{ \AA}$ with a 2θ range of $10\text{--}80^\circ$ and a scan rate of 0.02° per second. The morphology of the material was analyzed using SEM Jeol JSM-6510LA, Tokyo. The functional groups of the material were examined using a Shimadzu FTIR Spectrometer, Japan with a mid-infrared region ($4000\text{--}400/\text{cm}$). Data analysis and presentation of data results using the OriginLab program.

3 Results and Discussion

The diffraction pattern of the NMC811 oxalate product (NMC811 S-C2O4) is shown in Figure 2a. When compared with commercial NMC811, the diffraction pattern of NMC811 S-C2O4 is similar to that of commercial NMC811. NMC811 S-C2O4 was successfully obtained through the reaction of metal oxalates (nickel oxalate, manganese oxalate, and cobalt oxalate). Therefore, NMC811 S-C2O4 has the hexagonal $\alpha\text{-NaFeO}_2$ structure (space group R-3m). No secondary phases with detectable intensity were observed within the limits of laboratory-scale XRD detection, indicating that the oxalate-based solid-state reaction synthesis successfully yielded NMC811 material that is predominantly single-phase layered. Figure 3b shows the diffraction pattern of the NMC811 carbonate product (NMC811 S-CO3). NMC811 S-CO3 was successfully obtained through the reaction of metal carbonates (nickel carbonate, manganese carbonate, and cobalt carbonate). When compared with commercial NMC811, the [101] peak shifts and partially overlaps with the [006/102] doublet, while the [105] and [107] peaks exhibit significantly reduced intensities. Such features are commonly associated with structural disorder and partial degradation of layered ordering in Ni-rich NMC materials. Furthermore, an additional diffraction peak around 34°

was observed, which can be attributed to residual Li_2CO_3 as an impurity, indicating incomplete lithiation or carbonate decomposition during synthesis.

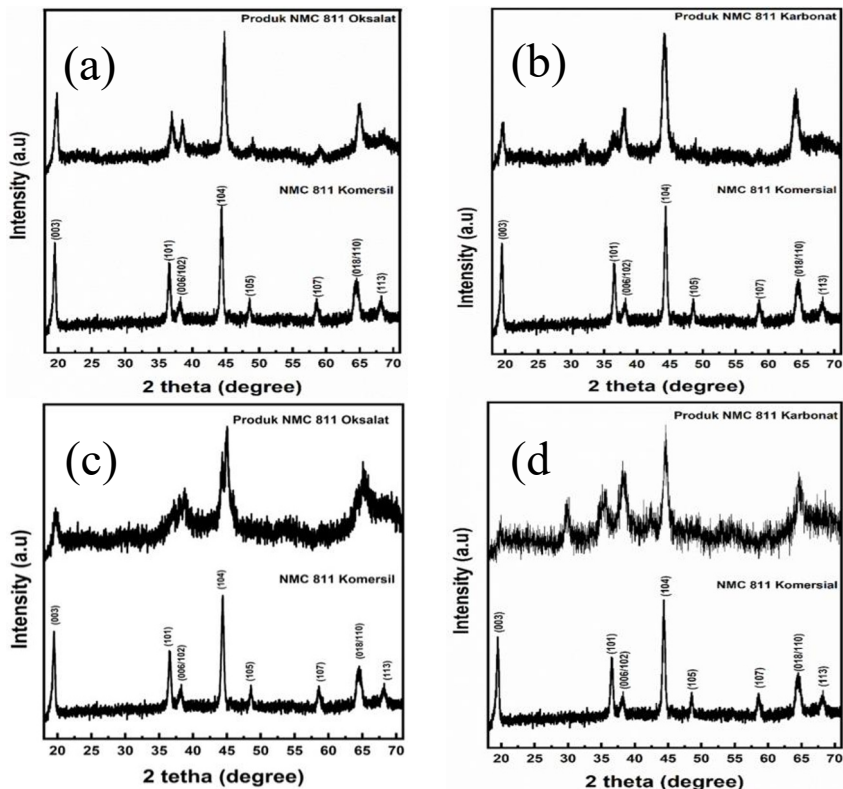


Fig. 2. X-ray Diffraction Pattern of NMC 811 (a) S-C2O4 (b) S-CO3 (c) M-C2O4 (d) M-CO3

The NMC811 oxalate product (NMC811 M-C2O4) and commercial NMC811 along with their respective diffraction patterns are shown in Figure 2c. NMC811 M-C2O4 was obtained through the reaction of metal oxalates (nickel oxalate, manganese oxalate, and cobalt oxalate). When the two diffraction patterns are compared, several peaks of NMC811 M-C2O4 are absent, such as the [101], [105], [107], and [113] peaks. This indicates that the layered R-3m structure is not fully developed in NMC811 M-C2O4 and that secondary phases or phases with poor crystallinity are present, along with impurities in NMC811 M-C2O4. Meanwhile, Figure 2d shows the diffraction patterns of the NMC811 carbonate product (NMC811 M-CO3) and commercial NMC811. NMC811 M-CO3 was obtained through the reaction of metal carbonates (nickel carbonate, manganese carbonate, and cobalt carbonate). If the two diffraction patterns are compared, several peaks of NMC811 M-CO3 are absent, such as the [105] and [107] peaks. This indicates that NMC811 M-CO3 does not have the hexagonal $\alpha\text{-NaFeO}_2$ structure (space group R-3m). In addition, NMC811 M-CO3 exhibits a peak around 32° , which indicates the presence of an impurity phase detected in the X-ray diffraction pattern of NMC811 M-CO3, namely Li_2CO_3 .

Overall, these results indicate that oxalate-based precursors, particularly via the solid-state reaction route, promote the formation of a more complete layered NMC811 structure compared to carbonate-based precursors. This behavior can be attributed to the cleaner thermal decomposition of metal oxalates, which facilitates improved cation homogeneity and lithiation during calcination, while carbonate precursors tend to yield residual lithium carbonate and structural disorder.

XRD analysis of the crystallite size for the NMC cathode material from each variation can be determined using the Debye-Scherrer equation, expressed in the following equation:

$$Dp = \frac{k\lambda}{B \cos \theta} \quad (1)$$

With, k = shape factor, or Scherer constant

λ = wavelength of X-rays

B = full width at half maximum (FWHM)

θ = diffraction angle

The (104) peak was chosen to determine the crystallite size as it appears across all NMC cathode materials. The results of the particle size calculation can be seen in Table 1:

Table 1. Crystal Size of NMC 811 Cathode Material

Sample	Crystal Diameter (nm)
NMC 811 Commercial	175,577
NMC 811 S-C2O4	171,972
NMC 811 S-CO3	128,628
NMC 811 M-C2O4	147,342
NMC 811 M-CO3	159,734

Based on Table 1, the commercial NMC cathode material has a crystallite diameter of 175.577 nm. Furthermore, when comparing NMC materials synthesized by various methods, the NMC produced via the solid-state oxalate method has a crystallite diameter closest to that of commercial NMC. Meanwhile, samples from the molten salt route exhibit smaller apparent crystallite sizes, which may be related to incomplete crystallization and residual impurities, not solely washing efficiency. It should be noted that the Debye–Scherrer method only provides a qualitative estimate of crystallite size, as it does not account for instrumental broadening or microstrain effects. Therefore, the observed differences in crystallite size should be interpreted as indicative trends rather than absolute values. Nevertheless, these results support the conclusion that the choice of precursor chemistry and synthesis route plays a critical role in controlling the crystallization behavior of Ni-rich NMC811 materials.

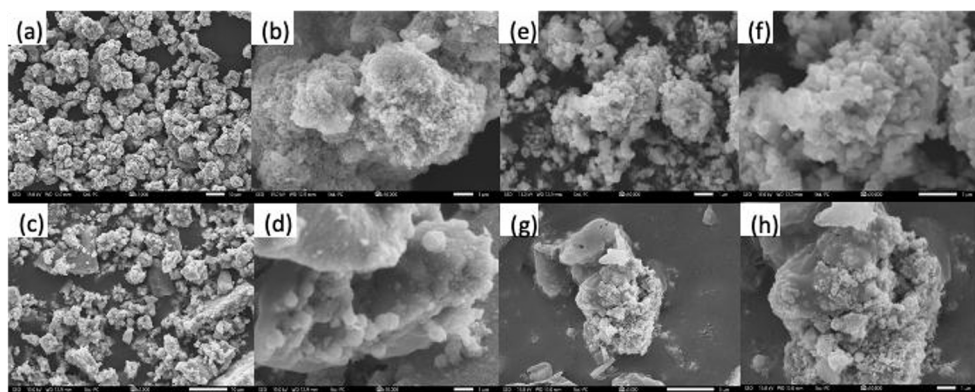


Fig. 3. Morphology of NMC 811 (a) S-C2O4 (b) S-CO3 (c) M-C2O4 (d) M-CO3

Figures 3(a) and 3(b) display scanning electron microscopy (SEM) images of solid-state synthesized oxalate-derived NMC811 (NMC811 S-C2O4), taken at magnifications of 1000× and 10,000×, respectively. At the lower magnification, the material is seen to consist of secondary particles that form micron-sized agglomerates (Figure 3(a)). A closer look at

higher magnification reveals that these agglomerates are actually made up of uniformly distributed primary particles. These primary particles have a nearly spherical shape and are sub-micron in size (Figure 3(b)). Small voids are also visible between the primary particles. These voids could potentially aid electrolyte infiltration and enhance lithium-ion transport within the secondary particle framework. The morphology of the solid-state carbonate-derived NMC811 (NMC811 S-CO₃) is presented in Figures 3(c) and 3(d) at 2000× and 10,000× magnification. Here, the secondary particles appear as irregular, micron-sized agglomerates (Figure 3(c)), while the primary particles largely retain a spherical form (Figure 3(d)). Compared to the oxalate-based sample, some of the secondary particle surfaces appear smoother. This smoother texture might suggest partial sintering occurred during the high-temperature calcination step, which could subsequently reduce the material's accessible surface area.

Moving to the molten salt method, the morphology of oxalate-based NMC811 (NMC811 M-C₂O₄) is shown in Figures 3(e) and 3(f). The images, taken at 10,000× and 20,000×, show secondary particles composed of spherical micron-sized agglomerates (Figure 3(e)). The primary particles, however, exhibit a more faceted, cube-like morphology and are relatively uniform in their sub-micron dimensions (Figure 3(f)). This improved uniformity can be linked to the role of molten NaCl. The salt melts around 800 °C, creating a liquid reaction environment that improves mass transfer, encourages consistent nucleation, and helps control excessive particle growth. Consequently, the molten salt route produces primary particles that are better dispersed and more uniform in size compared to the solid-state method. Finally, Figures 3(g) and 3(h) show the carbonate-based NMC811 synthesized via the molten salt route (NMC811 MCO₃) at 5000× and 10,000×. While the secondary particles remain as spherical micron-sized agglomerates (Figure 3(g)), the primary particles display highly irregular shapes. These include cubic, rod-like, and sheet-like structures (Figure 3(h)). This morphological diversity points to non-uniform nucleation and growth processes, likely resulting from incomplete decomposition of the carbonate precursors and localized compositional variations during the molten salt synthesis.

In summary, oxalate-based precursors consistently lead to more uniform primary particle morphology than their carbonate-based counterparts, regardless of the synthesis method employed. Furthermore, while the molten salt technique generally improves particle homogeneity, its effectiveness is more dependent on the precursor chemistry, as clearly seen in the case of carbonate-derived NMC811. While did not perform a quantitative analysis of the particle size distribution in this study, a qualitative review of the SEM images suggests that the oxalate-derived samples exhibit a narrower primary particle size distribution and more uniform particle shapes. These morphological traits are likely to enhance the material's effective surface area and shorten the diffusion pathways for Li⁺ ions. In practical terms, this could translate to better rate performance in battery applications.

Additionally, the structure seen in NMC811 S-C₂O₄ where uniformly packed primary particles are separated by small, consistent voids may improve mechanical stability during repeated charge-discharge cycles. This kind of architecture can better accommodate the volume changes that occur during lithium insertion and removal. In contrast, the irregularly shaped primary particles observed in the carbonate-derived, molten-salt samples could lead to localized stress build up. This stress concentration increases the likelihood of particle cracking and accelerated performance fade over extended cycling. A thorough investigation into how these specific morphological features correlate with electrochemical performance will be the focus of future work. This will involve systematic particle size distribution analysis, BET surface area measurements, and comprehensive electrochemical testing.

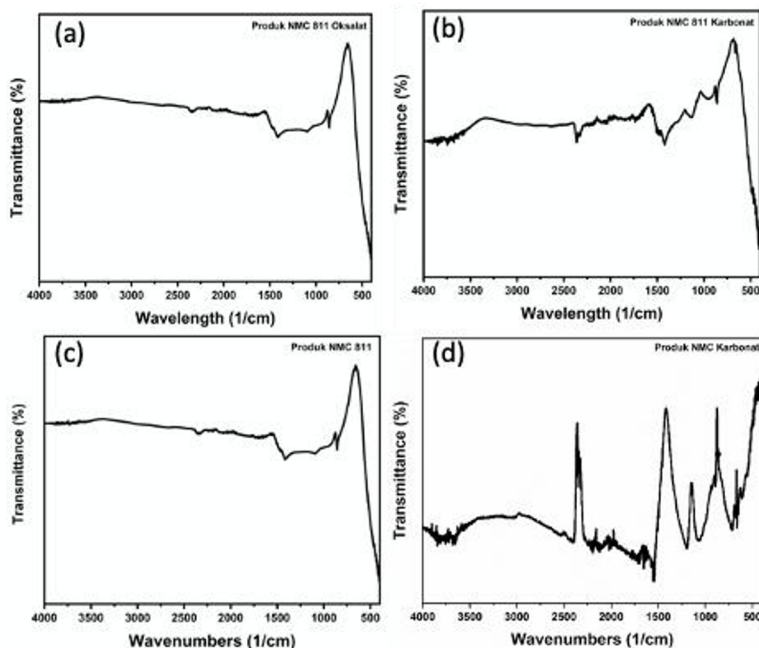


Fig. 4. Fourier Transform Infrared of NMC 811 (a) S-C2O4 (b) S-CO3 (c) M-C2O4 (d) M-CO3

Figure 4 presents the FTIR spectra of NMC 811 samples synthesized using different precursors and synthesis routes. FTIR analysis was used as a complementary technique to XRD to identify residual carbonate-related species that may not be clearly distinguishable from minor impurity phases in the diffraction patterns, particularly in nickel-rich layered oxides. Figure 4(a) shows the infrared absorption spectra of NMC811 S-C2O4. The peaks in the wavelength range of $\sim 2300/\text{cm}$ and $\sim 1300/\text{cm}$ indicate CO anions. This is attributed to the addition of an excessive Li^+ source, where residual Li^+ can react with atmospheric H_2O and CO_2 to form Li_2CO_3 . However, the intensity at this wavelength is not as large as NMC811 S-OH so the impurity composition of Li_2CO_3 smaller in NMC811 S-C2O4 compared to the NMC811 S-OH product. Figure 4(b) shows the infrared absorption spectra of NMC811 S-CO3. The peaks in the wavelength range of $\sim 2300/\text{cm}$ and $\sim 1300/\text{cm}$ indicate CO anions. This is also attributed to the addition of an excessive Li^+ ion source, leading Li^+ to react with water vapor and CO_2 in the air to form Li_2CO_3 . In addition, the CO anion can be caused by carbonate compounds that have not been completely decomposed during the fermentation process. The heating and washing process were less than perfect. Figure 4(c) shows the infrared absorption spectra of NMC811 M-C2O4. The peaks in the wavelength range of $\sim 2300/\text{cm}$ and $\sim 1300/\text{cm}$ indicate CO anions. This is attributed to an excessive Li^+ ion source, which is excessive, until Li^+ will react with water vapor and CO_2 in the air forming Li_2CO_3 . This is in accordance with the X-ray diffraction pattern which shows NMC811 M-C2O4 there is an impurity phase. Figure 69 shows the infrared absorption spectra of NMC811 M-CO3. This is consistent with the X-ray diffraction pattern showing NMC811 M-CO3. There is an impurity phase. The presence of the C-O group is indicated by a peak in the wavelength range between $\sim 1000/\text{cm}$ and $\sim 1200/\text{cm}$. In addition, the peak in the wavelength range of $\sim 1500/\text{cm}$ indicates the presence of the C=C group. This indicates the presence of the CO anion which is likely due to the presence of Li_2CO_3 or carbonate compounds that have not been completely decomposed during the heating process and the washing process is less than perfect. Overall, the FTIR analysis reinforces the XRD findings by confirming

that oxalate-based precursors facilitate more complete decomposition and the formation of a cleaner phase, whereas carbonate-based precursors are more susceptible to residual carbonate impurities. Although FTIR does not provide quantitative phase analysis, it serves as a sensitive probe for detecting carbonate related species and validates the impurity trends observed in the XRD data.

This study shows that the choice of precursor and synthesis method significantly affects the phase purity, crystallinity, and morphology of NMC 811 cathode material. XRD analysis confirmed that NMC 811 S-C2O4, synthesized by the solid-state method using oxalate precursor, has a hexagonal α -NaFeO₂ structure, which is clear without detectable impurities, very similar to commercial NMC 811. This indicates that oxalate facilitates more perfect decomposition and arrangement of cations during calcination. In contrast, carbonate-based samples (NMC 811 S-CO₃ and M-CO₃) show impurity phases, especially Li₂CO₃, which is caused by incomplete decomposition and residual carbonate groups. The molten salt method (NMC 811 M-C2O4) produces smaller crystallites (147.342 nm) than the solid-state synthesis (171.972 nm), indicating better nucleation due to the liquid-phase reaction environment. However, this method introduces impurities, as indicated by the FTIR peaks corresponding to unleached salt and Li₂CO₃.

Morphological analysis revealed that the oxalate precursor produced spherical primary particles with a uniform size distribution, while the carbonate precursor produced irregular shapes and agglomerates. The molten salt method improved particle dispersion but required more rigorous washing to remove salt residues, which is its main drawback. The presence of voids in the oxalate-based sample suggests potential benefits for electrolyte penetration, while the carbonate-based material exhibited a denser and less porous structure. These structural and morphological differences are crucial for electrochemical performance, as phase purity and particle homogeneity directly affect Li⁺ diffusion and cycle stability.

4 Conclusion

This study emphasizes the crucial role of precursor selection in the synthesis of NMC 811 cathode materials. Oxalate precursors, especially in solid-state synthesis, produce materials with better phase purity, hexagonal structure, and more uniform morphology that are close to commercial NMC 811. The molten salt method, although promising for particle homogeneity, in this study still requires further optimization to address impurity retention and washing efficiency. The presence of impurities and one of them is Li₂CO₃ the results of this study on carbonate-based samples underscore the importance of strict control over decomposition conditions. Future research should focus on refining molten salt synthesis parameters, exploring hybrid precursors, and evaluating electrochemical performance to bridge the gap between laboratory-scale synthesis and industrial applications. These advances will be key to developing high-performance NMC cathodes for next-generation lithium-ion batteries.

Acknowledgement

This research is supported by International Collaborative Research or KI-UNS (Grant Number: 369/UN27.22/PT.01.03/2025) and the Center for Excellence in Electrical Energy Storage Technology of Sebelas Maret University as a facility provider.

References

1. L. Xu *et al.*, ‘Progress in Preparation and Modification of LiNi_{0.6}Mn_{0.2}Co_{0.2}O₂ Cathode Material for High Energy Density Li-Ion Batteries’, *International Journal of Electrochemistry*, vol. **2018**, pp. 1–12, Jul. (2018), doi: 10.1155/2018/6930386.
2. X. L. Wang *et al.*, ‘Visualizing the chemistry and structure dynamics in lithium-ion batteries by in-situ neutron diffraction’, *Sci. Rep.*, vol. **2**, (2012), doi: 10.1038/srep00747.
3. Y. T. Tsai, C. Y. Wu, and J. G. Duh, ‘Synthesis of Ni-rich NMC cathode material by redox-assisted deposition method for lithium ion batteries’, *Electrochim. Acta*, vol. **381**, Jun. 2021, doi: 10.1016/j.electacta.2021.138244.
4. J. Han *et al.*, ‘Facile synthesis of Li-rich layered oxides with spinel-structure decoration as high-rate cathode for lithium-ion batteries’, *Electrochim. Acta*, vol. **299**, pp. 844–852, Mar. (2019), doi: 10.1016/j.electacta.2019.01.078.
5. M. Wang, Y. Han, M. Zhang, M. Chu, M. Liu, and Y. Gu, ‘Enhancing the electrochemical performance of Li-rich cathode material by a flexible precursor treatment method’, *Solid State Ion.*, vol. **357**, Dec. (2020), doi: 10.1016/j.ssi.2020.115498.
6. P. Zhang *et al.*, ‘Synergistic Na⁺ and F⁻ co-doping modification strategy to improve the electrochemical performance of Li-rich Li₁₋₂₀Mn₀₋₅₄Ni₀₋₁₃Co₀₋₁₃O₂ cathode’, *Ceram. Int.*, vol. **46**, no. 15, pp. 24723–24736, Oct. (2020), doi: 10.1016/j.ceramint.2020.06.263.
7. G. Sun *et al.*, ‘In-situ surface chemical and structural self-reconstruction strategy enables high performance of Li-rich cathode’, *Nano Energy*, vol. **79**, Jan. (2021), doi: 10.1016/j.nanoen.2020.105459.
8. X. Yao *et al.*, ‘Oxalate co-precipitation synthesis of LiNi_{0.6}Co_{0.2}Mn_{0.2}O₂ for low-cost and high-energy lithium-ion batteries’, *Mater. Today Commun.*, vol. **19**, pp. 262–270, Jun. (2019), doi: 10.1016/j.mtcomm.2019.02.001.
9. X. Wan, W. Che, D. Zhang, and C. Chang, ‘Improved electrochemical behavior of Li rich cathode Li_{1.4}Mn_{0.61}Ni_{0.18}Co_{0.18}Al_{0.03}O_{2.4} via Y₂O₃ surface coating’, *Mater. Charact.*, vol. **169**, Nov. (2020), doi: 10.1016/j.matchar.2020.110602.
10. F. I. Saaid *et al.*, ‘Ni-rich lithium nickel manganese cobalt oxide cathode materials: A review on the synthesis methods and their electrochemical performances’, Jan. 15, 2024, *Elsevier Ltd.* doi: 10.1016/j.heliyon.2023.e23968.
11. M. Malik, K. H. Chan, and G. Azimi, ‘Review on the synthesis of LiNi_xMn_yCo_{1-x-y}O₂ (NMC) cathodes for lithium-ion batteries’, Aug. 01, (2022), *Elsevier Ltd.* doi: 10.1016/j.mtener.2022.101066.
12. X. Yao *et al.*, ‘Oxalate co-precipitation synthesis of LiNi_{0.6}Co_{0.2}Mn_{0.2}O₂ for low-cost and high-energy lithium-ion batteries’, *Mater. Today Commun.*, vol. **19**, pp. 262–270, Jun. (2019), doi: 10.1016/j.mtcomm.2019.02.001.
13. M. Di Veroli *et al.*, ‘Coprecipitation–driven memory effect: Linking precursor precipitation conditions to NMC811 cathode performance’, *J. Power Sources*, vol. **665**, p. 239058, Feb. 2026, doi: 10.1016/j.jpowsour.(2025).239058.
14. A. K. Tyagi and R. S. Ningthoujam Editors, ‘Indian Institute of Metals Series Handbook on Synthesis Strategies for Advanced Materials Volume-I: Techniques and Fundamentals’. [Online]. Available: <http://www.springer.com/series/15453>
15. T. Wang *et al.*, ‘Reciprocal Ternary Molten Salts Enable the Direct Upcycling of Spent Lithium-Nickel-Manganese-Cobalt Oxide (NMC) Mixtures to Make NMC 622’.